# Chemistry–A European Journal

Supporting Information

## Mesoporous $CuFe_2O_4$ Photoanodes for Solar Water Oxidation: Impact of Surface Morphology on the Photoelectrochemical Properties

Marcus Einert,* Arslan Waheed, Dominik C. Moritz, Stefan Lauterbach, Anna Kundmann, Sahar Daemi, Helmut Schlaad, Frank E. Osterloh, and Jan P. Hofmann

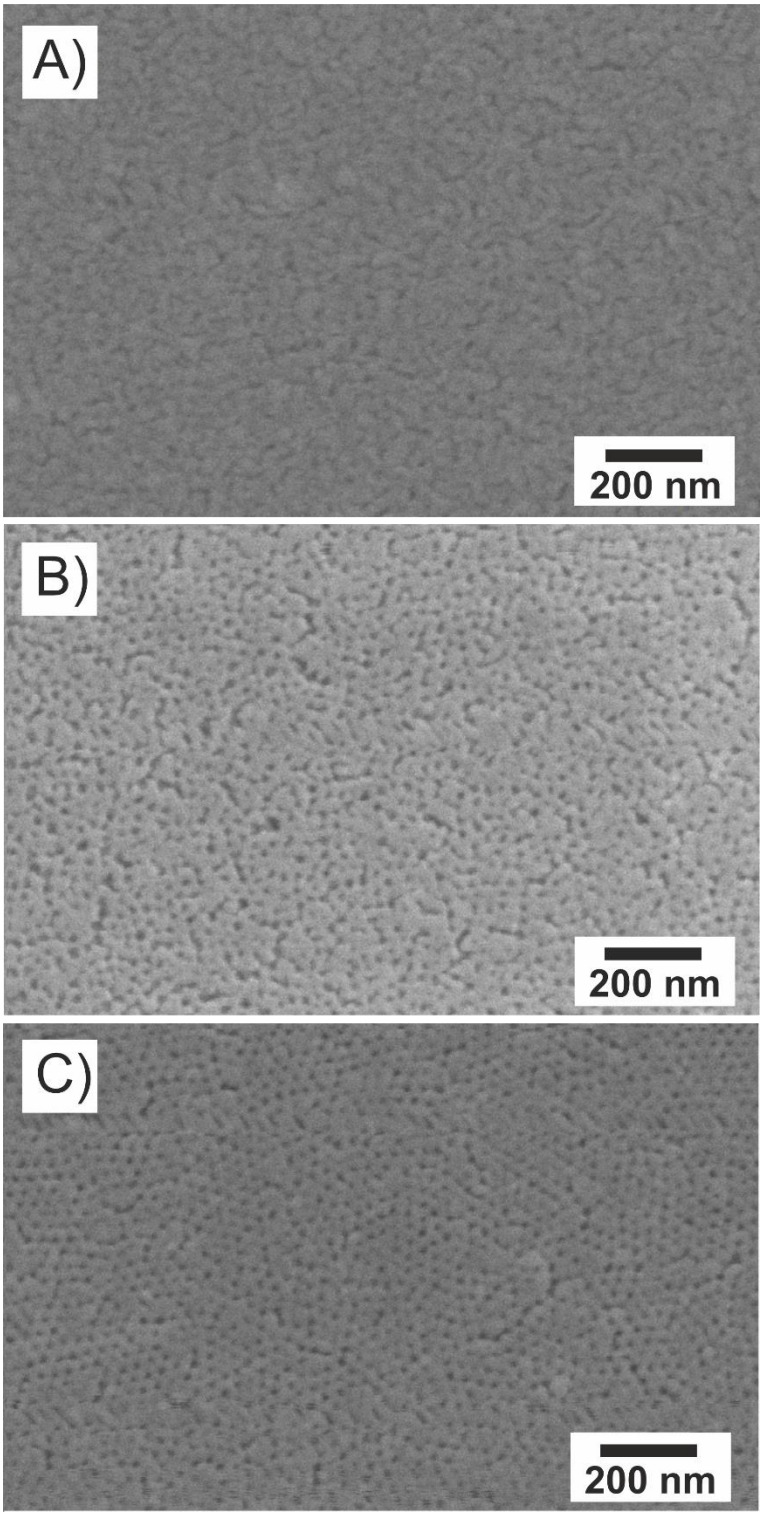


**Figure S1.** SEM images of the A) CFO-F127, B) CFO-PIB, and C) CFO-KLE thin films annealed at 600 °C for 10 min.

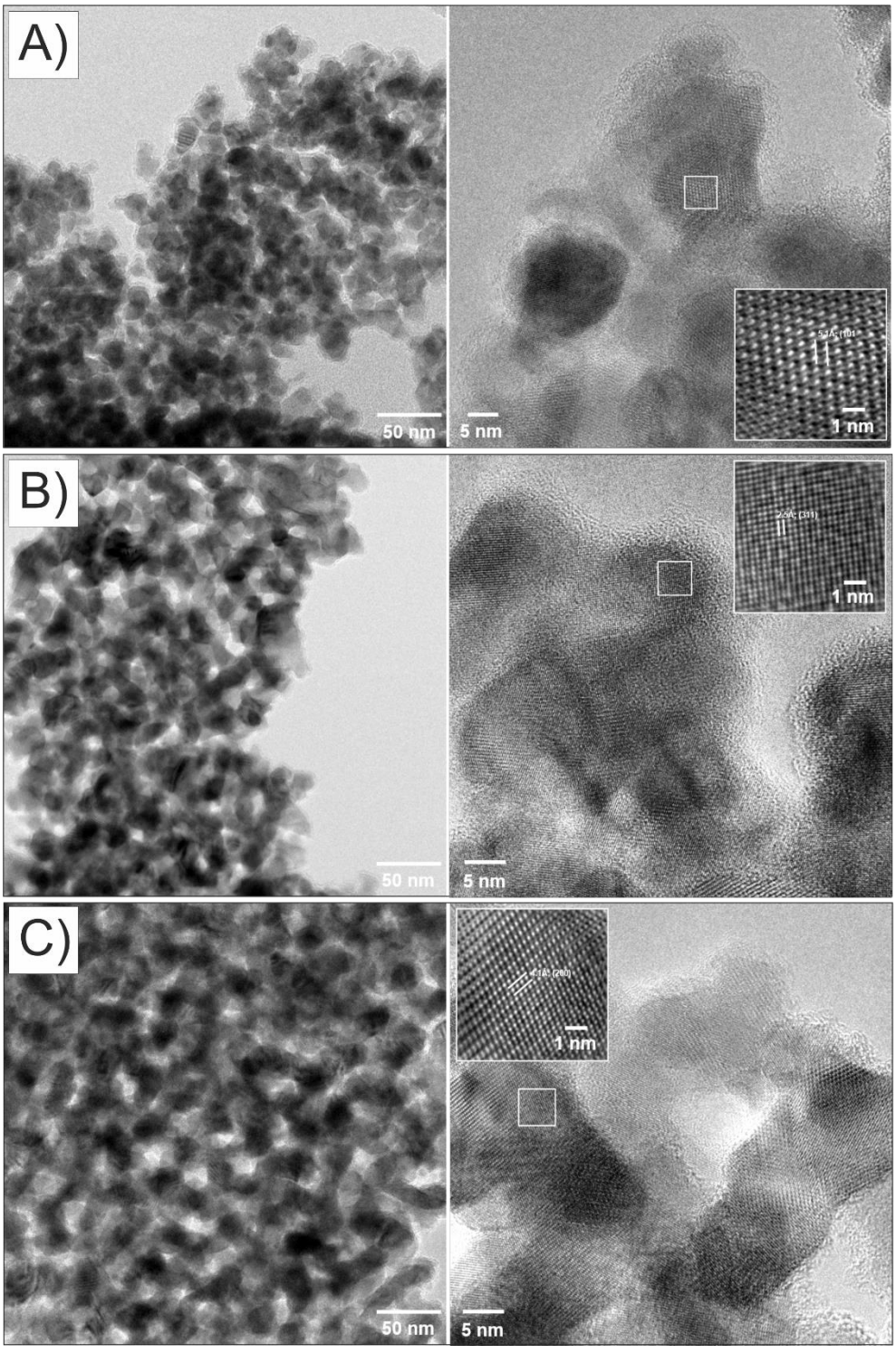


**Figure S2.** Bright-field TEM pictures (left) in high resolution (right) including insets showing iFFT filtered images of the HRTEM images illustrating the lattice plane spacing of the tetragonal spinel structure A) $d_{101}$ for CFO-F127, B) $d_{311}$ for CFO-PIB, C) $d_{200}$ for CFO-KLE.

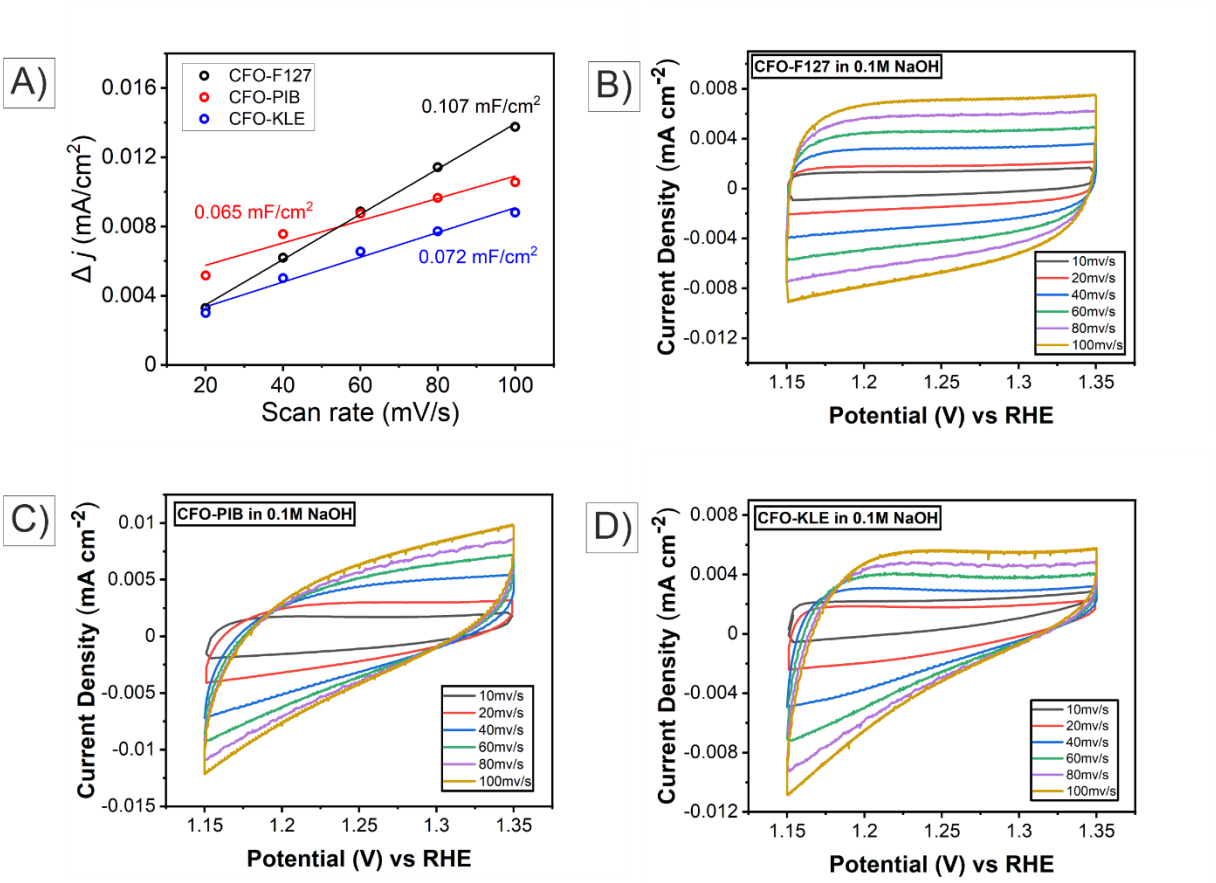


**Figure S3.** A) Differential current densities and the corresponding specific double-layer capacities, $C_{DL}$, determined by linear fitting of the data points. CV sweeps of B) CFO-F127, C) CFO-PIB, and D) CFO-KLE calcined at 600 °C recorded for distinct scan rates from 10 mV/s to 1000 mV/s. All electrochemical experiments were conducted in 0.1 M NaOH and in a 3-electrode set-up.

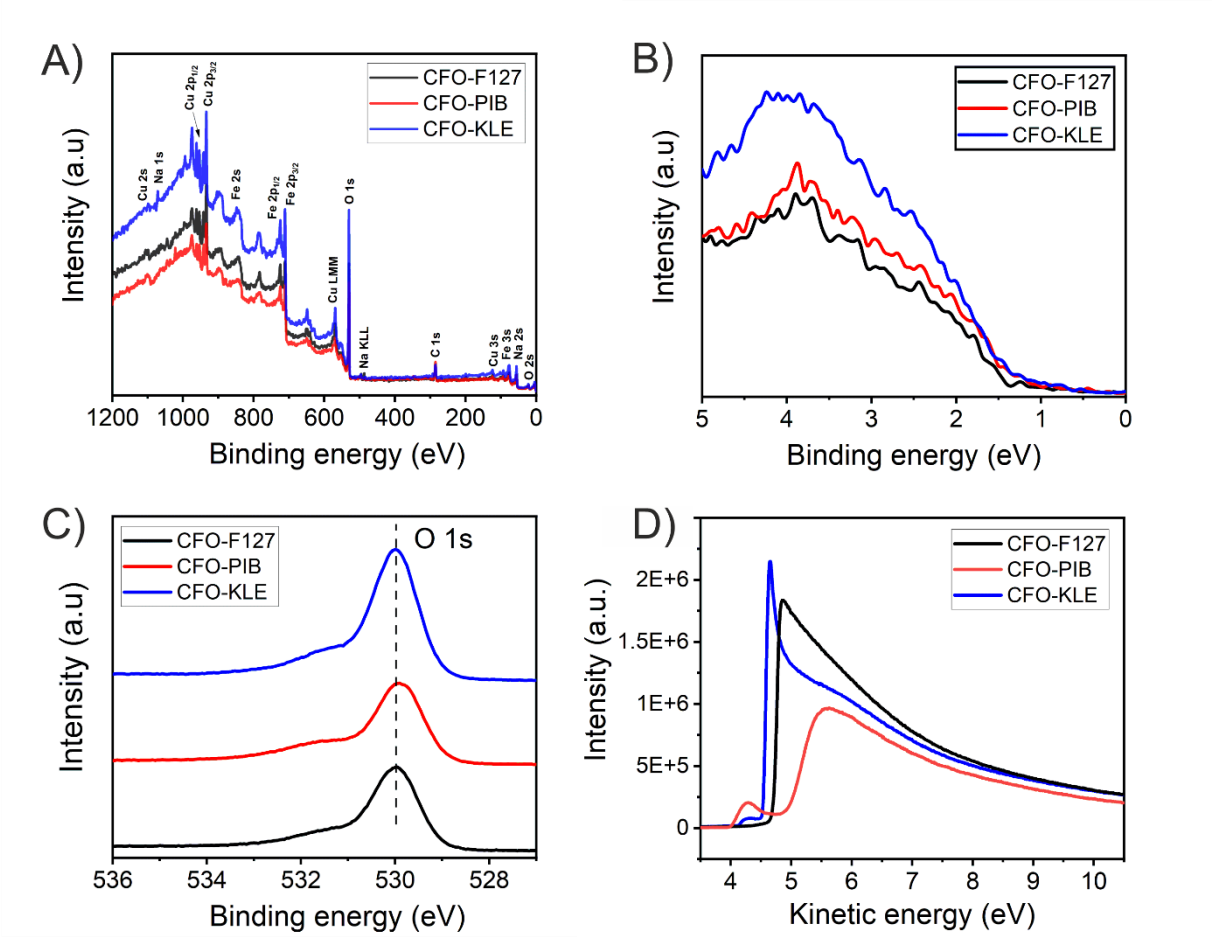


**Figure S4.** A) XPS survey spectra, B) fine-scan spectra of the O 1s emission lines of the CFO-F127 (black), CFO-PIB (red), and CFO-KLE (blue). C) XPS valence band spectra recorded for binding energies between 0 and 5 eV. D) Secondary cut-off potentials with an applied bias of – 3V.

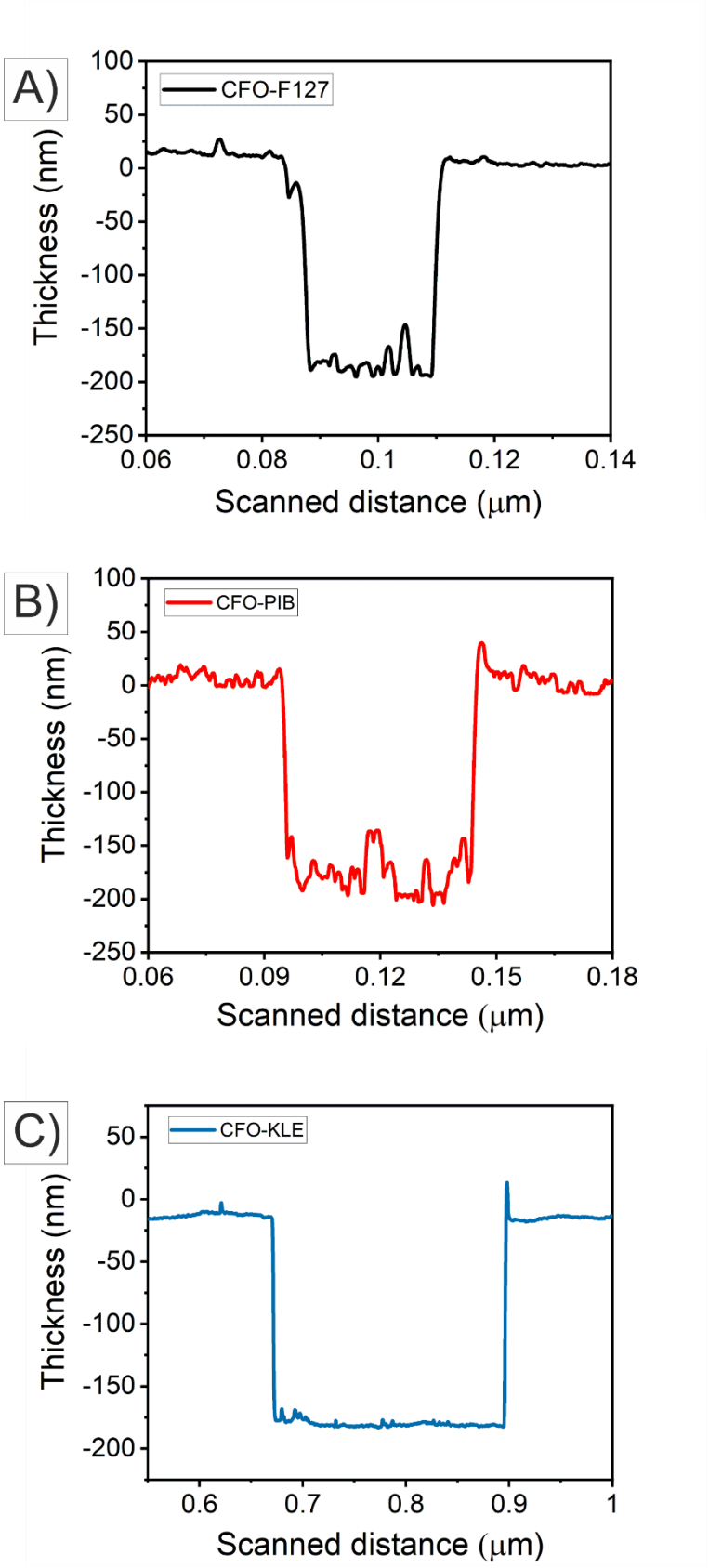


**Figure S5.** Determination of the film thickness by profilometry for the A) CFO-F127, B) CFO-PIB, and C) CFO-KLE samples calcined at 600 °C.

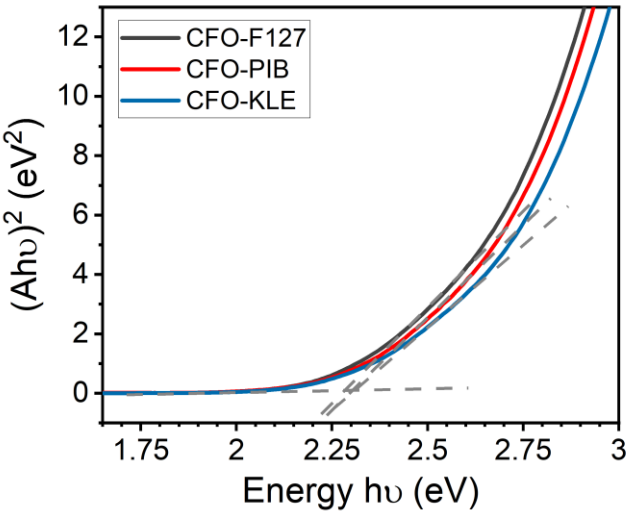


**Figure S6.** Tauc plots for direct optical transitions of the CFO-F127, CFO-PIB, and CFO-KLE thin films. The grey dotted lines serve as guidance for the eye for estimation of the band gap energies.

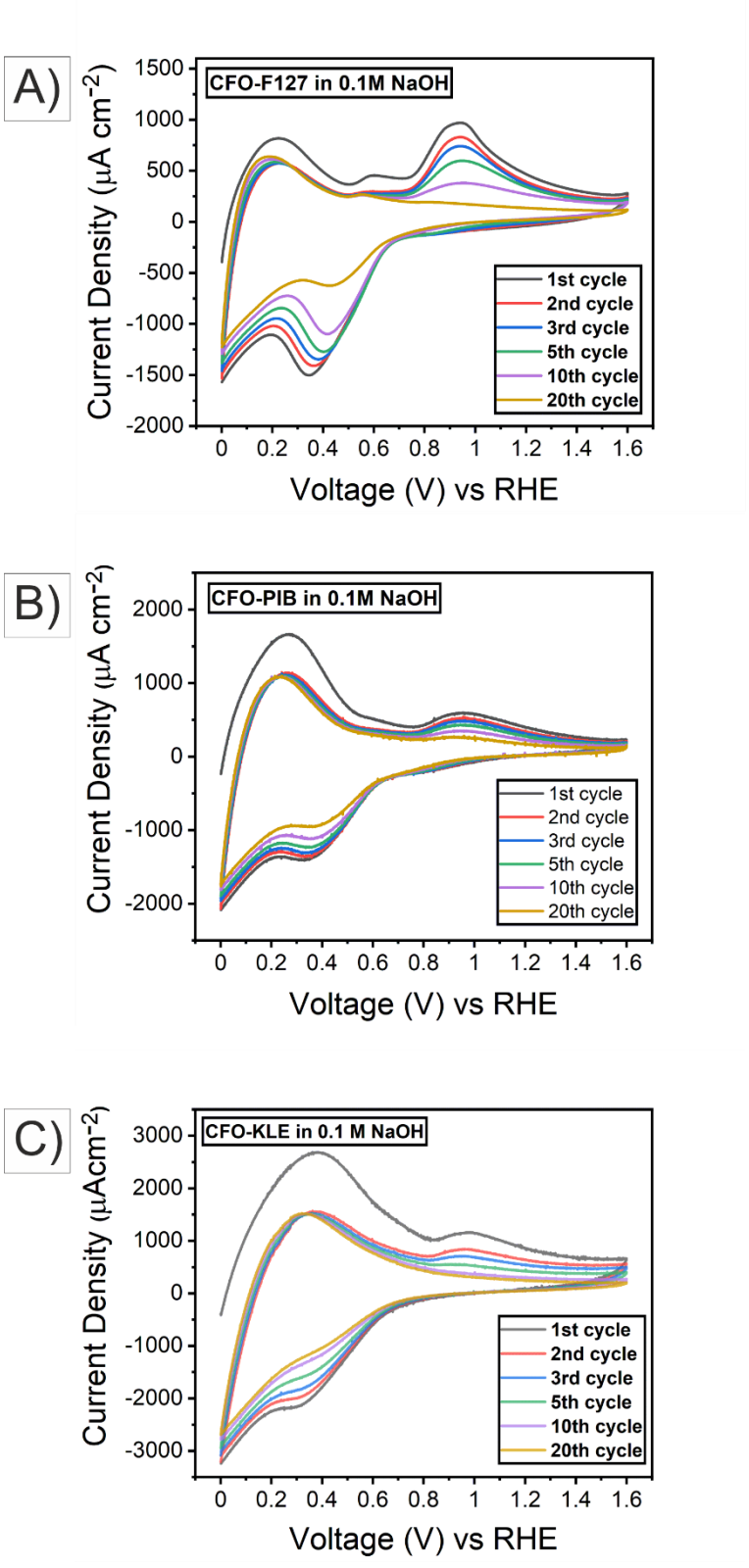


**Figure S7.** 20 consecutive cyclic voltammetry curves measured for A) CFO-F127, B) CFO-PIB, and C) CFO-KLE between 0 V and 1.6 V vs. RHE in 0.1 M NaOH (pH 12.9) with a scan rate of 50 mV/s.

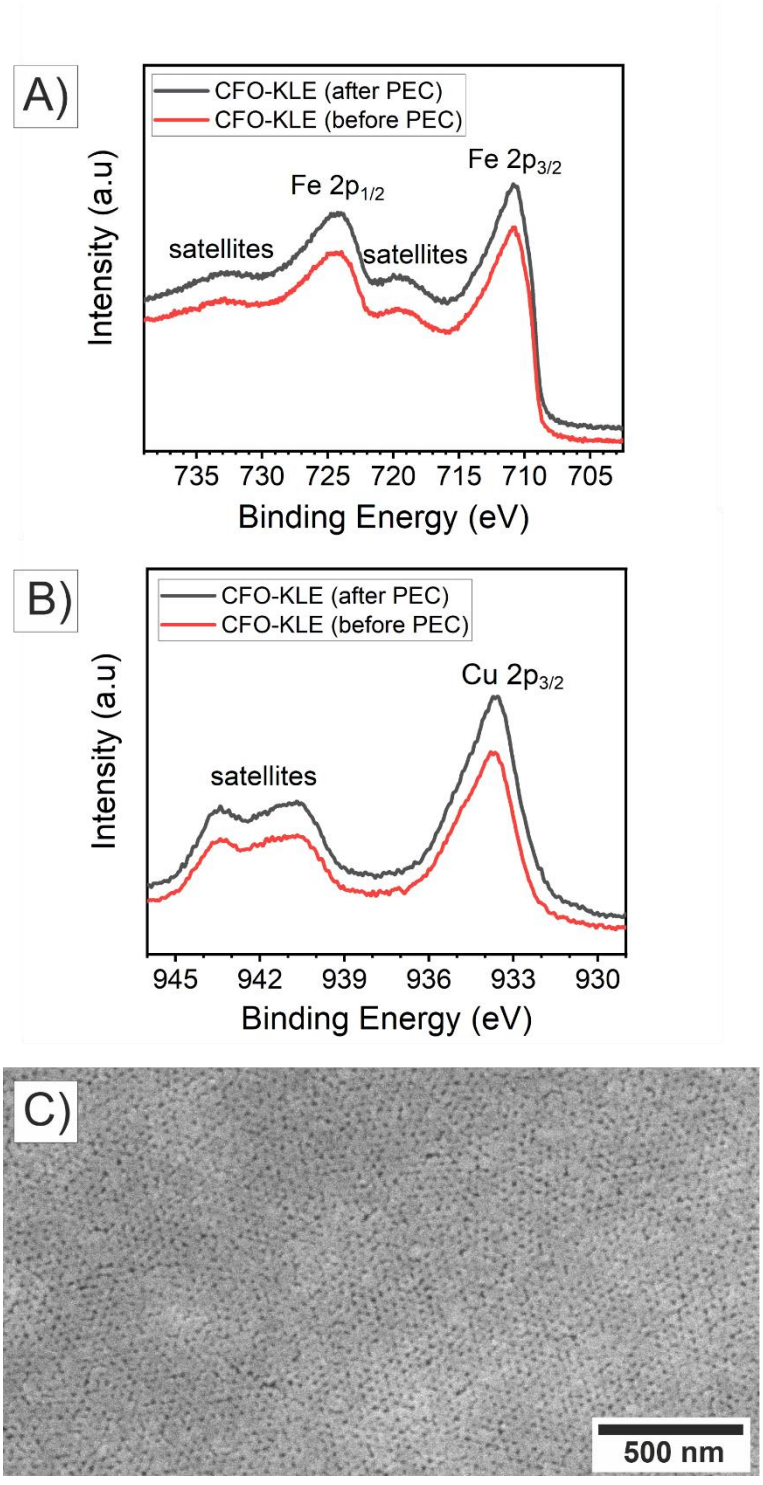


**Figure S8.** A) Fe 2p core level spectra and B) Cu 2p core level spectra of the CFO-KLE samples before (red) and after PEC analysis (black). C) SEM image of the mesoporous CFO-KLE thin film after PEC analysis.

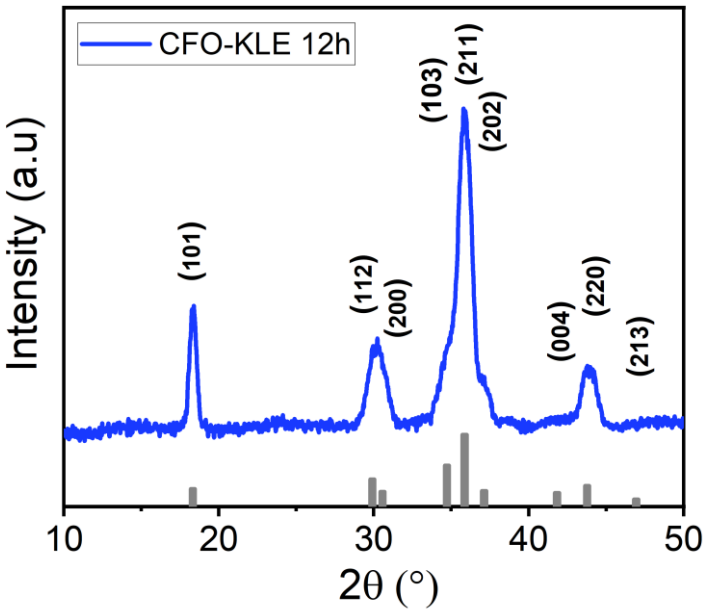


**Figure S9.** GI-XRD diffraction patterns of the 12 h calcined CFO-KLE thin films and reference bars (grey) according to JCPDS no. 034-0425 indicative for the tetragonal spinel phase.

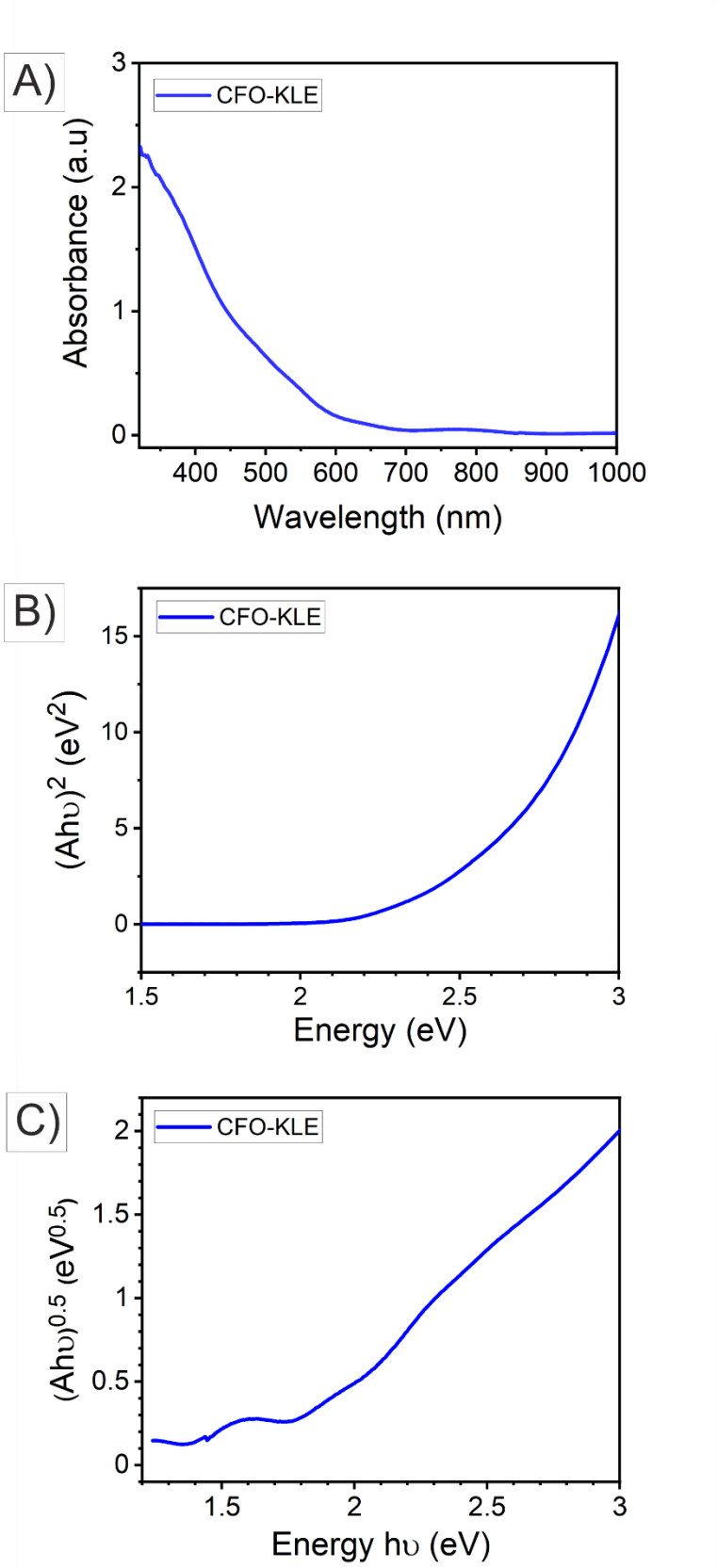


**Figure S10.** A) Absorbance spectra, B) Tauc plot for a direct optical transition, and C) Tauc plot for an indirect optical transition for the CFO-KLE samples calcined for 12 h at 600 °C.

**Mott-Schottky equation:**

$$\frac{1}{C^2} = \frac{2}{e\varepsilon\varepsilon_0 N_D A^2} \cdot \left(V - V_{Fb} - \frac{k_B T}{e}\right) \quad \text{(E1)}$$

$1/C_{SC}^2$ can be plotted as function of the applied potential and then the flat band potential can be derived by ascertaining the intercept on the x-axis. $N_D$ is the donor density, $C$ the capacitance of the space charge layer, $\varepsilon$ the dielectric constant of the semiconductor, $\varepsilon_0$ the vacuum permittivity, $A$ the surface area of the exposed electrode, $V$ the applied voltage, $V_{FB}$ the flat band potential, $e$ the elementary charge, $k_B$ the Boltzmann constant, and $T$ the temperature.

**Optimization of PEC performance**

Since not only the calcination temperature, but also the holding time has been demonstrated to have major impact on the photoelectrochemical properties of metal oxide-based photoelectrodes due to extensive increase of crystallinity, the mesoporous CFO thin films were also photoelectrochemically characterized after prolonged annealing time. All synthetic parameters were kept otherwise constant except of the calcination holding time, which was changed from 10 min to 12 hours at 600 °C. Because any change in surface morphology upon/after sintering at this elevated temperature can be ideally detected on well-ordered surface morphologies, again, we chose the ordered mesoporous CFO-KLE samples as control sample. Figure 9 A shows the SEM image of the CFO-KLE thin film calcined for 12 h. The images show that the increase in holding time changed the pore morphology significantly due to sintering of nanocrystals within the pore walls also resulting in a breakdown of the ordered mesoporous framework. Interestingly, even after 12 h calcination, separated mesopores with well-developed cylindrical shapes were sporadically still present. The GI-XRD pattern (Figure S9) demonstrates more pronounced and intense peaks compared to the Bragg signals observed in the diffractograms for the 10 min calcined CFOs. All peaks can be indexed according to the tetragonal spinel phase (JCPDS 034-0425). The 12 h calcined CFO-KLE samples possess drastically enhanced photocurrent densities of 0.37 mA/cm$^2$ compared to the 0.18 mA/cm$^2$ of the 10 min calcined CFO counterpart by almost doubling the photocurrent density when measured at 1.3 V *vs.* RHE in 0.1 M NaOH containing 1 M $Na_2SO_3$. Since the absorption of light was not enhanced for the 12 h (Figure S10) compared to 10 min calcined CFO-KLE samples (Figure 3), the improved PEC response is most likely attributed to the increase of crystallinity and the development of larger CuO domains possessing less defect sites. The 12 h calcined CFO films were further compared in terms of comparing distinct excitations sources.

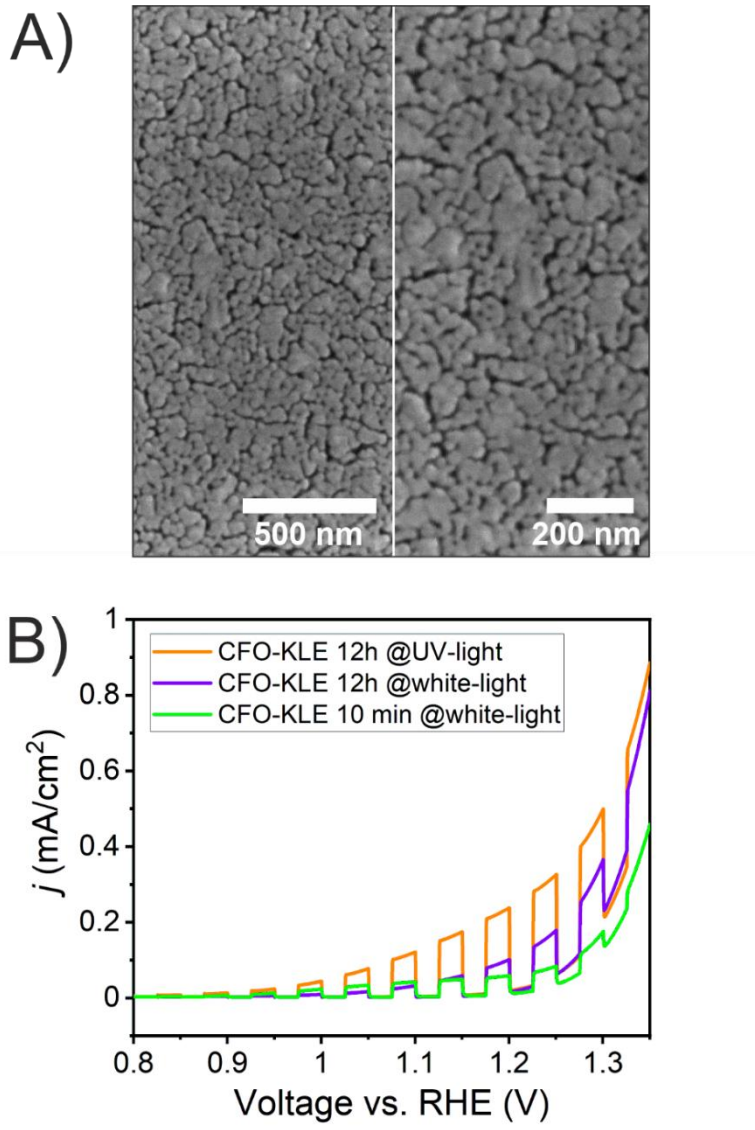


**Figure S11.** Characterisation of the CFO-KLE thin films treated at 600 °C for 12 h: A) SEM images in low (left) and high magnification (right), and C) intermittent-light voltammetry operated with UV-light LED (λ = 365 nm, orange line), a white-light LED (violet line). The performance of the 10 min calcined CFO-KLE illuminated with a white light LED is shown for comparison (green line). All experiments were conducted in 0.1 M NaOH (pH 12.9).

Therefore, the CFO materials were investigated through a white-light LED (100 mW/cm$^2$, $\lambda_{max}$ = 562 nm) and a UV-light LED (100 mW/cm$^2$, $\lambda_{max}$ = 369 nm) both possessing the same illumination intensity (corresponding to the solar spectral irradiance AM 1.5e G). The CFO-KLE films irradiated with UV-light exhibit photocurrent densities of 0.3 mA/cm$^2$ and 0.5

$mA/cm^2$ at 1.23 V and 1.3 V *vs.* RHE, respectively, which was found to be as a substantial increase of 35% when compared to the PEC performance of CFO samples illuminated with a white-light LED (Figure 7 C). The significant difference in PEC performance can be ascribed to the absorption of high-frequency photons from the UV-source, which will be absorbed by the CFO-KLE samples to a much larger extent compared to low-energy photons. At an excitation wavelength of 369 nm every photon possesses enough and even more energy (369 nm corresponds to 3.36 eV) to excite an electron-hole pair above the band edges of the CFO-KLE (band gap energies were found to be 1.6 eV and 2.3 eV for direct and indirect transitions, respectively, compare Figure 3 B and S6). In essence, electrons and holes can also be photoexcited to sub-conduction and sub-valence band states (energetically much higher than near-band-edge states), respectively. These hot charge carriers are known to relax to near-band-edge states or directly react with the specific redox species (from the electrolyte), explaining the enhanced photoresponse observed for UV-irradiated CFO samples.